



# **iJRASET**

International Journal For Research in  
Applied Science and Engineering Technology



---

# **INTERNATIONAL JOURNAL FOR RESEARCH**

IN APPLIED SCIENCE & ENGINEERING TECHNOLOGY

---

**Volume: 6      Issue: III      Month of publication: March 2018**

**DOI: <http://doi.org/10.22214/ijraset.2018.3589>**

**[www.ijraset.com](http://www.ijraset.com)**

**Call: ☎ 08813907089**

**E-mail ID: [ijraset@gmail.com](mailto:ijraset@gmail.com)**

# Synthesis of Perovskite Phase Strontium Substituted Cerium Ferrites for its Photocatalytic Application

Ashwini Anantharaman<sup>1</sup>, V. Mary Teresita<sup>2</sup>, B. Avila Josephine<sup>3</sup>, T.L Ajeesha<sup>4</sup>, Mary George<sup>5</sup>

<sup>1,4</sup>Research Scholar, <sup>2,3</sup>Assistant Professor <sup>5\*</sup>Associate Professor, Department of Chemistry, Stella Maris College, Chennai-600086, India

**Abstract:** Perovskites prepared in nanoscale have recently received extensive attention as the inorganic perovskite-type oxides are fascinating materials due to their wide range of applications as catalysts, solid-oxide fuel cells, sensors and so on. In the current study, sol-gel method was applied and the corresponding metal nitrates were used as precursors for the preparation of pure and mixed cerium strontium ferrites in perovskite phase. The materials were sintered at 800°C for 8 hours to obtain in nanoscale. Substitution in A or B site of  $ABO_3$  perovskite structure modifies the properties of the materials. The structural, optical and magnetic properties of the as synthesized materials were investigated using PXRD, FT-IR, UV-DRS, TEM and VSM techniques. The photo catalytic activity of the synthesized nano materials using the cationic methylene blue dye indicated higher degradation efficiency of about 97% for mixed ferrite compared to pure oxides.

**Keywords:** Sol-gel, Perovskite, Ferrites, Magnetic, Photo catalytic.

## I. INTRODUCTION

Perovskites are mixed metal oxides with the general formula  $ABO_{3\pm\delta}$  where A is rare earth ion and B can be alkaline earth metal or transition metal ion. Partial substitution of A and B ions can lead to the formation of variety of compounds with general formula  $A_{1-x}A_xB_{1-y}B'_yO_{3\pm\delta}$  due to non-stoichiometry.

Rare-earth ferrites have a tilted orthorhombic structure as the cation sites are highly substitutable which helps in modifying the properties such as: conductivity, pyroelectric, piezoelectric, magneto-optic, ferro-electric, magnetic for studying the specific applications of perovskite [1-10]. Several methods employed for nanomaterial synthesis include sol-gel, co-precipitation, solid-state sintering, and combustion route [11, 12].

Extensive modifications of the structural and magnetic properties were observed on substituting  $Sr^{2+}$  and  $La^{3+}$  in  $La_{1-x}Sr_xFeO_{3-\delta}$  in comparison with pure  $LaFeO_3$  perovskite where there is no magnetic interaction between  $Fe^{3+}$  and  $La^{3+}$  as  $La^{3+}$  is non-magnetic in nature [13].

Saeid Jabbarzare et.al reported on the synthesis of cerium ferrite perovskite and investigated for the magnetic, photocatalytic, absorption and dielectric properties which indicated  $CeFeO_3$  as a ceramic with good colossal dielectric constant.  $SrFeO_{3-\delta}$  was prepared by sol-gel route to study the conductivity and see back measurements. Shivendra Kumar Jaiswal et.al [14] synthesized via sol-gel route produced highly stable anion deficient strontium ferrite which acts as a filter for air with excellent oxygen permeation characteristics [15].

Therefore, an attempt has been made here to synthesize cerium strontium ferrite perovskite via sol-gel method. Further, in addition pure oxides, cerium strontium oxide and cerium ferrite were compared with the mixed novel ferrite by thoroughly analyzing the optical, structural and magnetic properties of the synthesized materials.

## II. EXPERIMENTAL DETAILS

### A. Synthesis of perovskite oxides

For the synthesis of pure and mixed nano ferrites, appropriate amounts of cerous nitrate, strontium nitrate and ferric nitrate were used as precursors. Initially, citric acid was dissolved in ethylene glycol and was placed in magnetic stirrer at 150°C for 15 minutes. The nitrate solutions on mixing with the above solution on continuous stirring gave rise to gel which was digested for 3 hours at 250°C. The solid mass obtained was subsequently sintered in muffle furnace at 800°C for 8 hours to produce fine powders as the final product.

### B. Photo Catalytic Studies

In the present work cationic dye (methylene blue) of 25ppm stock solution and 0.1g of pure and mixed ferrite nano materials were used as photo catalyst 2mmol of fenton's reagent was also used. Photocatalytic activity was assessed from the degradation of methylene blue dye solution where, the reaction was carried out in HEBER multi-lamp photo reactor system. The degradation studies were done both in the presence and absence of UV lamp irradiation for 180minutes. The progress of the reaction was monitored by drawing the sample for every 30minutes and determining the absorbance from UV visible spectrometer

## III. RESULTS AND DISCUSSION

### A. X-Ray Diffraction Analysis

The XRD patterns of molar compositions of  $\text{CeSr}_{1-x}\text{Fe}_x\text{O}_{3-\delta}$  ( $x=0, 0.5$  and  $1$ ) oxides were sintered at  $800^\circ\text{C}$  are presented in fig.1. The grain sizes were calculated from the most intense peak from Debye Scherrer formula and found to be 39 nm, 23 nm and 28 nm for CSFO1( $\text{CeSrO}_{3-\delta}$ ), CSFO2( $\text{CeSr}_{0.5}\text{Fe}_{0.5}\text{O}_{3-\delta}$ ) and CSFO 3( $\text{CeFeO}_{3-\delta}$ ) respectively. All the three 6m6olar compositions showed particle size less than 100nm and the formation of single phase perovskite. CSFO2 matches with slight variations in the  $2\theta$  values which find the novelty of mixed metal perovskite. Therefore, the structure of synthesized nano materials were of orthorhombic symmetry which is in-line with the JCPDF no: 82-2427 for cerium strontium oxide (CSFO1) and JCPDF no: 22-0166 for cerium ferrite. The decreased crystalline size confirms that the synthesized materials are nano crystalline in nature.

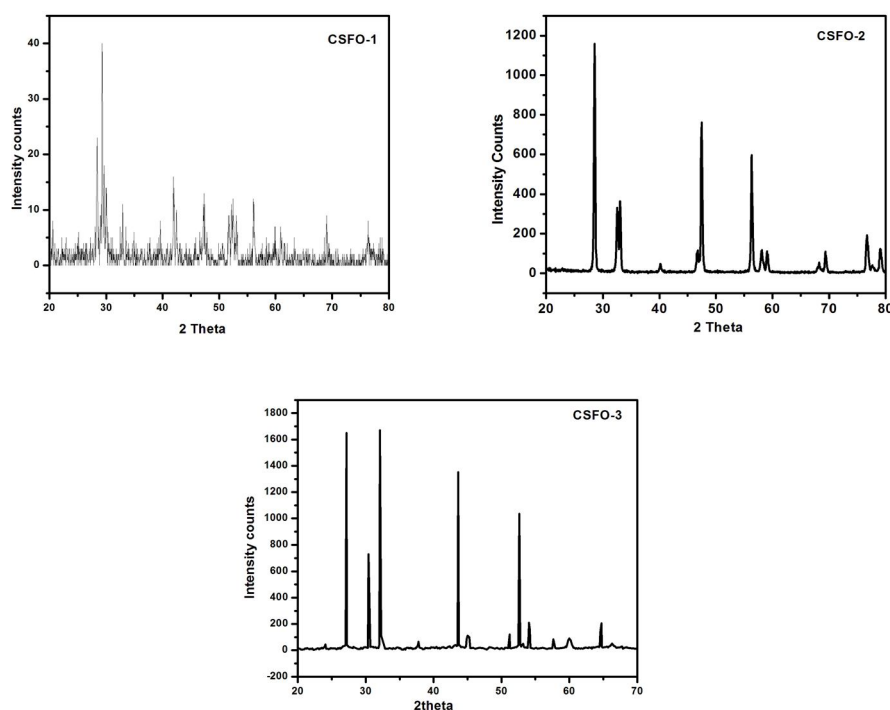


Fig.1. X-Ray diffractograms of CSFO1- CSFO3 nano materials

### B. FT-IR Analysis

FT-IR was used to determine the surface functional groups present in the synthesized nanomaterials. The infra-red spectra of the pure (CSFO-1 and CSFO-3) and mixed ferrite (CSFO-2) are represented in fig.2. The peaks around  $850\text{cm}^{-1}$  and  $480\text{cm}^{-1}$  for  $\text{CeSr}_{1-x}\text{Fe}_x\text{O}_{3-\delta}$  ( $x=0, 0.5$  and  $1$ ) confirm the formation of perovskite type oxides. The broad band around  $3400\text{cm}^{-1}$  is indicative of free and hydrogen bonded hydroxyl groups absorbed by the nano materials. The metal-oxygen stretching frequencies associated with the vibrations of Ce-O, Sr-O and Fe-O bonds are obtained in the range of  $400-900\text{cm}^{-1}$  exists as mixed metal perovskite oxides.



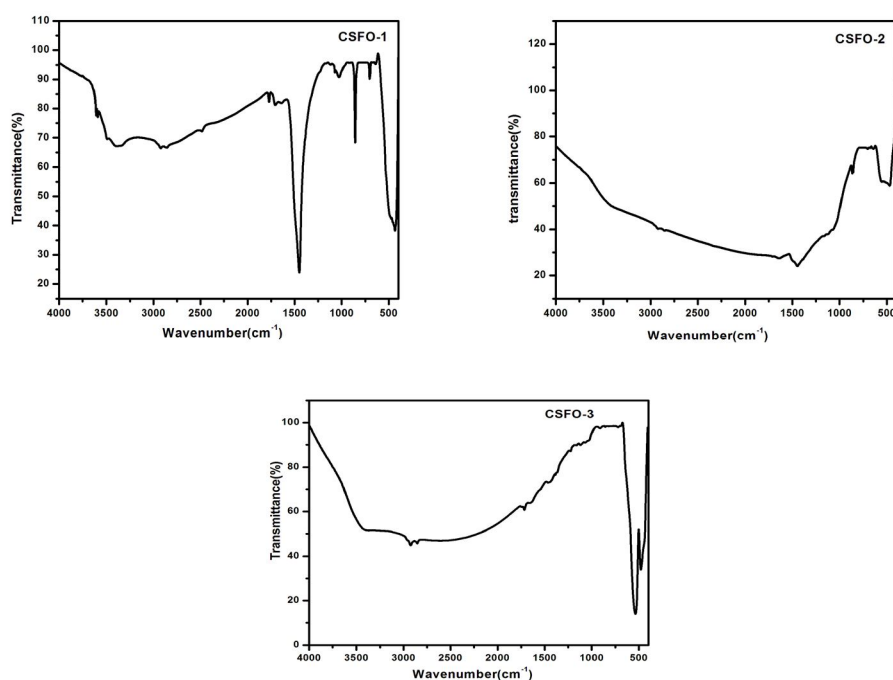
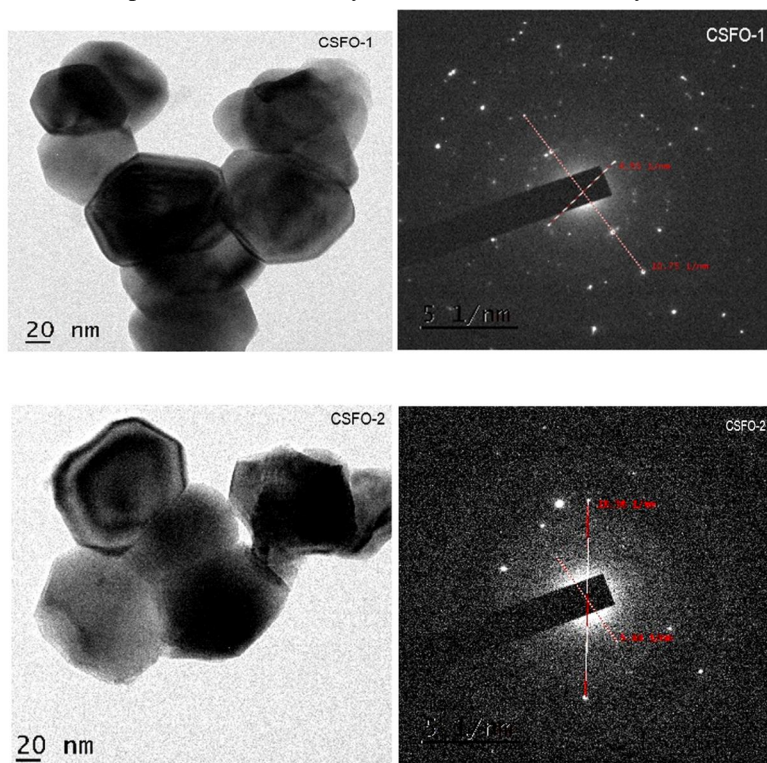


Fig.2. FT-IR spectra of CSFO1-CSFO3 nano materials

### C. TEM Analysis

The surface morphology of the synthesized nano materials was analysed using high resolution TEM technique. TEM and SAED images are displayed in Fig.3. The images showed the presence of large agglomerates with irregular shapes. The bright spots with the ring in the electron diffraction patterns reveal the crystalline nature of all the synthesized nano materials.



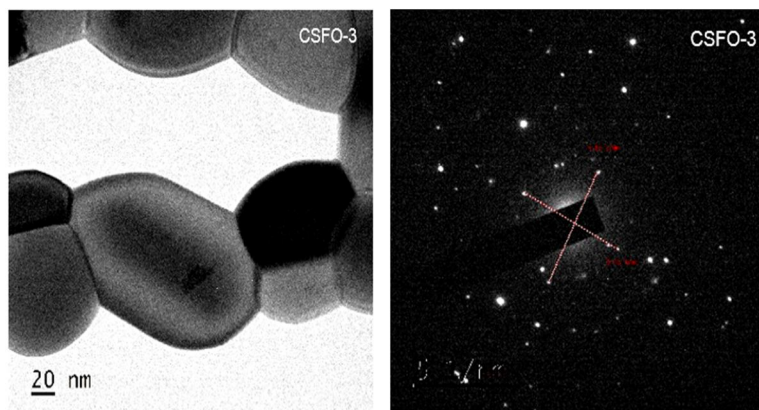


Fig.3. TEM and SAED images of CSFO1-CSFO3 nano materials

#### D. Optical Analysis

The optical absorption spectra of the synthesized pure and novel mixed ferrite are represented in fig.1. Pure cerium strontium oxide (CSFO 1) contains an absorption band centered around wavelength of about 334nm with 3.71 eV might be due to charge transfer transition. Iron containing 3d electrons interacts strongly with surrounding oxygen anions giving rise to localized states. The band gap energy was calculated using the relation  $E_g = hc/\lambda$  where  $\lambda$  is known as cut-off wavelength and  $h$  is the plank's constant. The absorption peaks observed at 321nm (CSFO 2) and 334 nm (CSFO 3) with band gap value 3.81 eV and 3.71 eV correspond to the ligand to metal charge transition. The maximum absorption bands at 690 nm and 660 nm for mixed perovskite (CSFO 2) and pure ferrite ( CSFO 3) are related to the energy gap of 1.79 eV and 1.87eV which might be due to the octahedral field splitting between  $t_{2g}$  and  $e_g$  of iron orbitals. These energy values can also be attributed to the crystal field charge transfer within  $Fe^{3+}$  ions. Therefore, the spectra showed red shift as the maximum absorbance has shifted to the longer wavelength in the band gap transition and are in agreement with the visible light absorptivity which enables its use as a semiconducting photocatalysts for photodegradation applications.

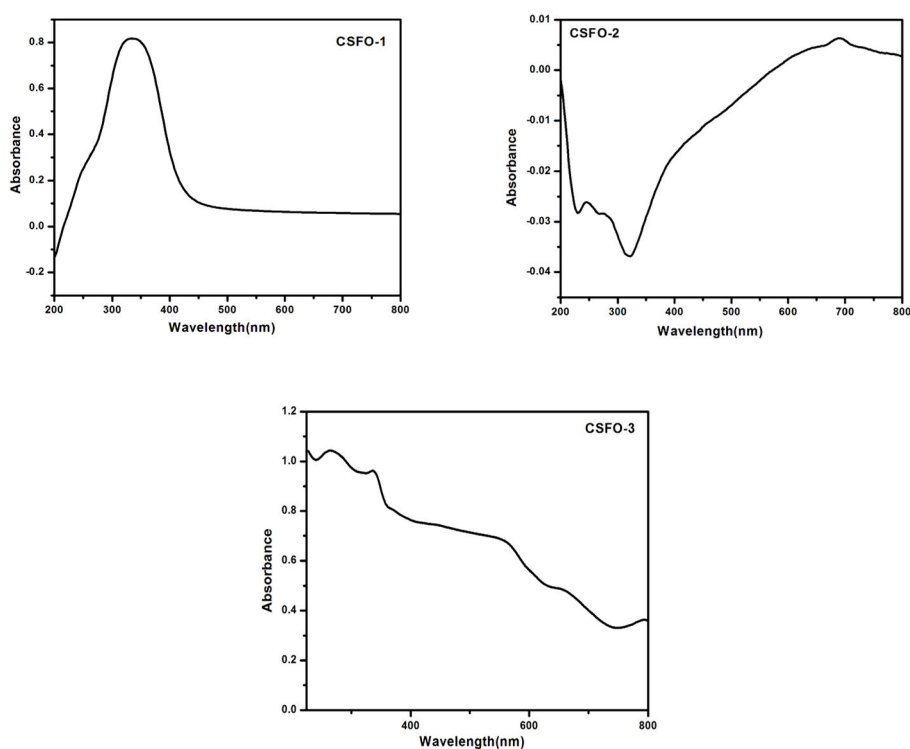


Fig. 4. UV-Visible spectra of CSFO1-CSFO3 nano materials

### E. Magnetic Analysis

Magnetic properties in the inorganic solid materials are due to the inclusion of ions with unpaired d and f electrons. Fig.5 showed the hysteresis loops for the pure (CSFO 1 and CSFO 3) oxides and mixed metal oxide (CSFO 2). The shape of the hysteresis loops indicated weak ferromagnetic behaviour. The magnetization is not saturating with higher coercivity of 6814Oe which is characteristic for antiferromagnetic ordering of spins in mixed metal ferrite (CSFO 2). The large value of coercivity is because of the finite size effect and high magneto crystalline anisotropy. The magnetic property increases upon substitution of strontium content. The weak ferromagnetism is as a result of spin canting that arose from tilted  $\text{FeO}_6$  octahedral. Inclusion of large sized  $\text{Sr}^{2+}$  cations reduces Fe-O bond and strengthens the antiferromagnetic super exchange ordering. The presence of oxygen vacancies is also important as it disturbs super exchange interactions thereby increasing ferromagnetism. In addition, the uncompensated surface spins also contribute to increase in magnetization of nanomaterials. The magnetic measurements of the synthesized nanomaterials are presented in table.1.

Table.1 Magnetic measurements of CSFO1 – CSFO3 nanomaterials

Nanomaterials	CSFO-1	CSFO-2	CSFO-3
Coercivity ( $H_{ci}$ )	548.44 G	6814.9G	3645.0 G
Magnetization( $M_s$ ) emu	404.65E-6	43.130E-3	3.9366E-3
Retentivity ( $M_r$ ) emu	76.303E-6	23.011E-3	1.6682E-3
Squareness ratio	0.1885	0.533	0.4237

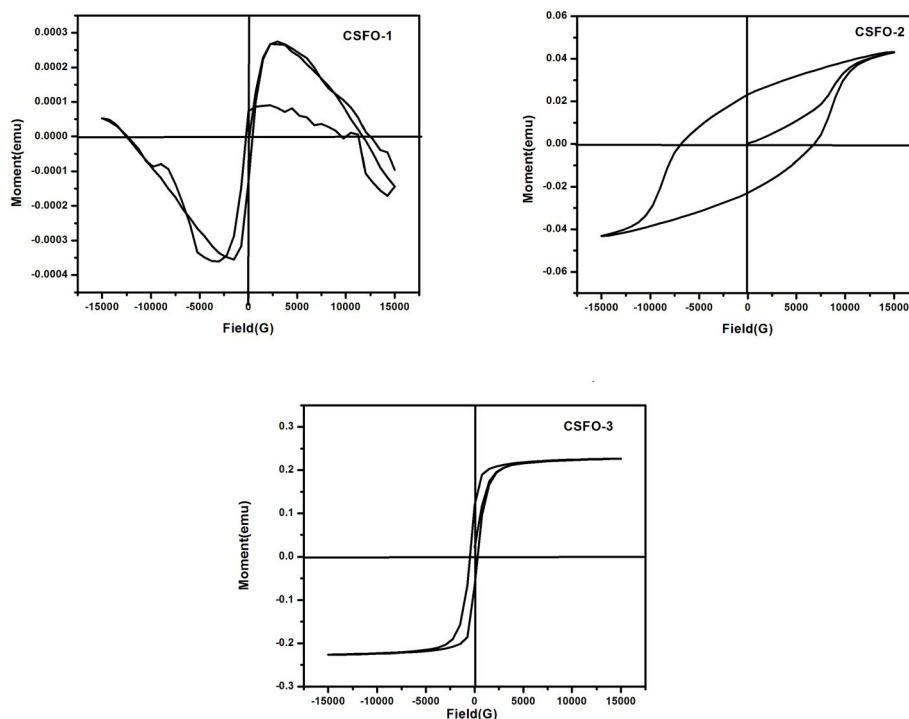


Fig. 5. Magnetization curves for CSFO1-CSFO3 nano materials

### F. BET Analysis

The adsorption-desorption isotherms and pore size distributions curves of  $\text{CeSr}_{1-x}\text{Fe}_x\text{O}_{3-\delta}$  ( $x=0, 0.5$  and  $1$ ) oxides are showed in fig.6. All the synthesized perovskite oxide displayed type II isotherm with large deviation from Langmuir model. The intermediate flat region in the isotherm corresponds to monolayer formation. Due to the reduced particle size, they are classified as mesoporous nanomaterials.

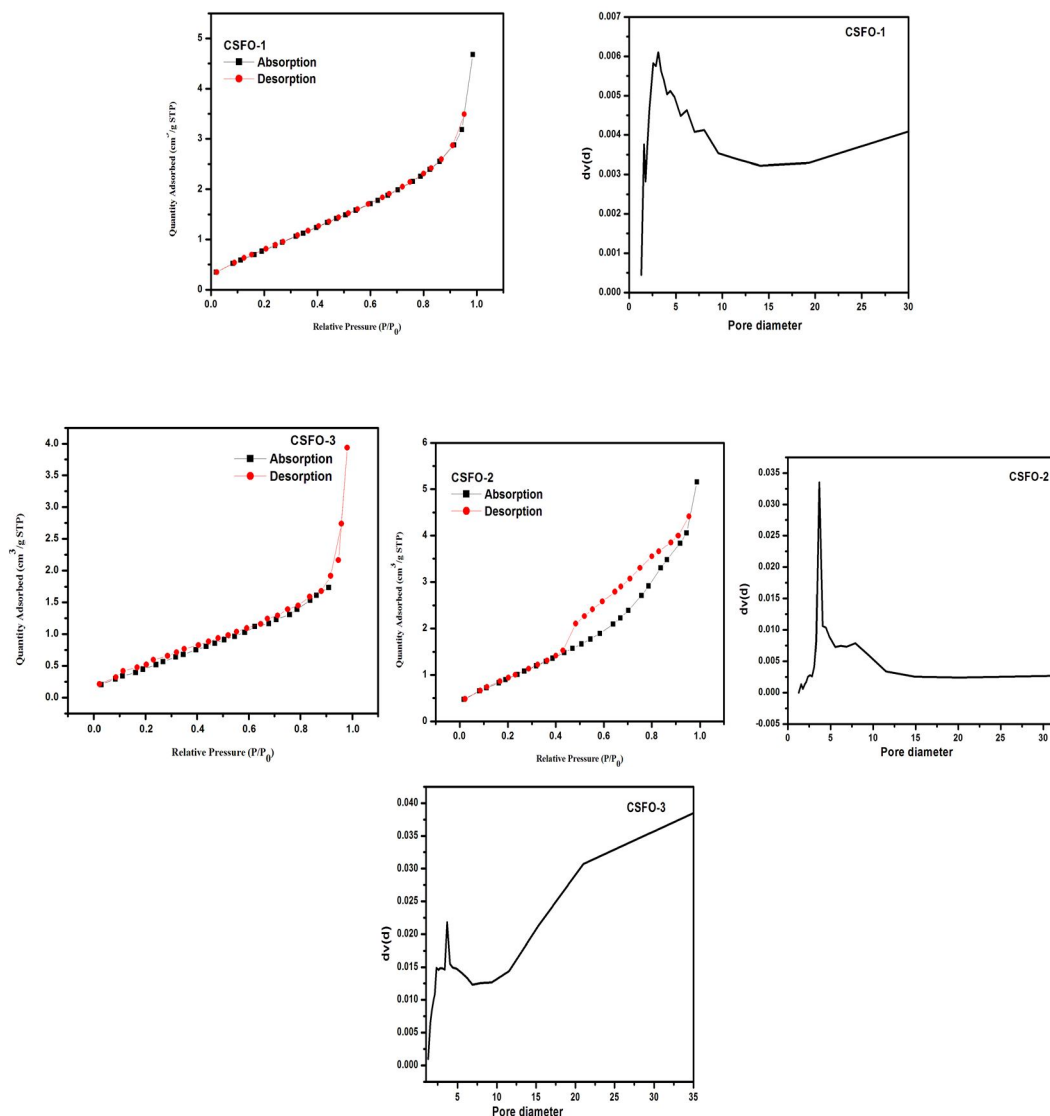


Fig. 6. BET isotherms and pore size distribution curves of CSFO1-CSFO3 nano materials

### G. Photocatalytic Studies

The maximum absorption of methylene blue dye solution is observed at 663 nm. The absorption peak decreased with increased time upon UV-lamp irradiation. Chromophores which imparts colour to the dye were broken down and thus methylene blue was degraded. The decreased particle size in nanometer scale might be the reason for the photodegradation property of the catalyst. Addition of fenton's reagent played a vital role as it behaved as an electron acceptor and undergoes decomposition to produce OH radicals. Electron acceptor is being added in the reaction to avoid electron-hole recombination which showed positive effect on degradation activity of the catalysts. The preliminary reactions carried out resulted in very low degradation activity both in presence and absence of light. The dark reaction on addition of fenton's reagent showed 1%, 4.5% and 1.35% for CSFO 1 – CSFO3 respectively. The reduction in absorption bands on increasing time under UV-lamp illumination was as observed in fig.7.

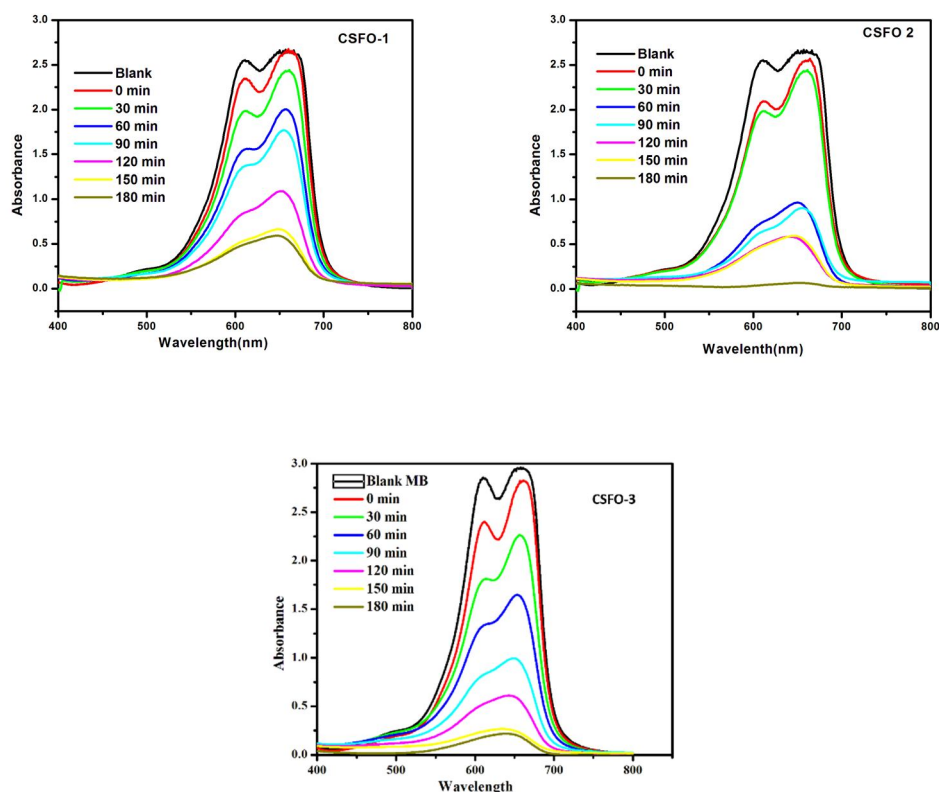


Fig.7. Absorption curves of CSFO1-CSFO3 nano materials

- 1) *Kinetics and degradation efficiency of photocatalysts:* The photodegradation of methylene blue dye in the presence of semiconductor catalysts followed pseudo first order kinetics. A linear fit plot was obtained as represented in fig.8. The photo degradation efficiency of the synthesized nanomaterials were compared as shown ion fig.9. Higher degradation activity was observed due to smaller particle size which was confirmed from XRD and TEM analysis. It was clearly noted from the figure that strontium substituted mixed perovskite (CSFO 2) exhibited 97% catalytic efficiency due to oxygen vacancies compared to pure (CSFO 1and CSFO 3) perovskite oxides.

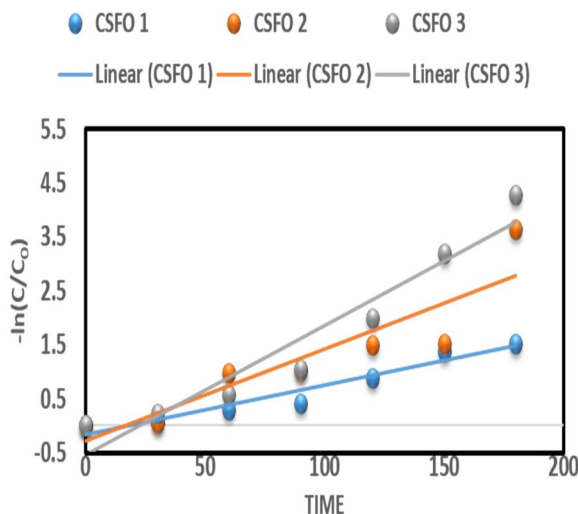


Fig. 8. Linear kinetic plot for CSFO1-CSFO3 nano materials



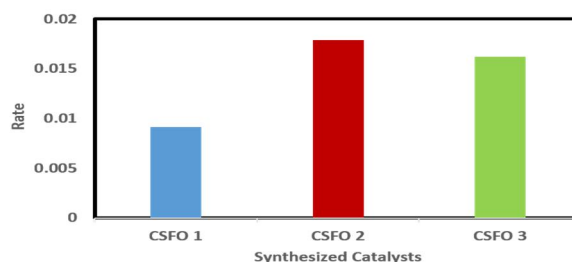


Fig.9. Degradation efficiency of the synthesized photocatalysts.

#### IV. CONCLUSIONS

In the present work, we describe the synthesis of crystalline mixed metal perovskite oxides of formula  $\text{CeSr}_{1-x}\text{Fe}_x\text{O}_{3-\delta}$  ( $x=0, 0.5$  and  $1$ ) via sol-gel route and its importance as photocatalysts in photodegradation applications. XRD pattern confirmed the single phase orthorhombic symmetry with particle decreased crystallite size for all the synthesized materials. TEM micrographs displayed large agglomeration with indefinite shapes. Optical absorption studies clearly describe the synthesized nanomaterials as semiconductors and its usage as a catalyst in visible light region. The hysteresis loops indicated weak ferromagnetic behaviour which resulted in spontaneous magnetization when an external field is applied. BET analysis indicated type II isotherm as the surface area had a favourable effect leading to degradation efficiency of the nanomaterials. 97% degradation efficiency was achieved for mixed perovskite oxide (CSFO 2) compared to pure oxides and further, these oxide materials could be used as catalysts in industries.

#### V. ACKNOWLEDGMENTS

The authors sincerely thank the analytical services rendered by DST-FIST Lab, Centre for Research in Science and Technology (CRIST), Stella Maris College (Autonomous), Chennai and Sophisticated Test & Instrumentation Centre (STIC) Cochin University of Science and Technology Cochin - 682 022, Kerala, India.

#### REFERENCES

- [1] Kubacka, M. Fernández-García and G. Colón, "Advanced nano architectures for solar photocatalytic applications", Chem. Rev., Vol 112, pp. 1555, Mar. 2012
- [2] D. M Schultz and T. P Yoon, "Solar synthesis: prospects in visible light photocatalysis", Science., Vol 343, pp.123917, Feb.2014.
- [3] N. Wang, D. Kong and H. He, "On the sol-gel synthesis and characterization of strontium ferrite ceramic Material", Powder Technol., Vol 207, pp. 470, Dec.2011
- [4] B Zhan, J. L Lan, Y. C Liu, Y. H Lin and C W Nan, "Enhanced thermoelectric properties of Pb-doped BiCuSeO ceramics", J. Inorg. Mater., Vol 29, pp. 237, Dec.201
- [5] I. E Wachs and K. Routray, "Fundamental Characterization Studies of Advanced Photocatalytic Materials ", ACS Catal., Vol 2, pp.1235, Jan.2012.
- [6] R. A. Eichel, " correlations between the nonstoichiometry and the Thermodynamic data of perovskite-type compounds in the La-sr-Mn-o system" Phys. Chem. Chem. Phys., Vol 13, pp. 368, Mar.201
- [7] J. Suntivich, H. A Gasteiger, N. Yabuuchi, H. Nakanishi, J. B. Goodenough and Y. Shao-Horn, " Design principles for oxygen-reduction activity on perovskite oxide catalysts for fuel cells and metal-air batteries", Nat. Chem., Vol 3, pp. 546, Dec.201
- [8] J. B Good Enough, "Bond-length fluctuations and the spin-state transition in  $\text{LCoO}_3$  ( $\text{L}=\text{La, Pr, and Nd}$ )", Rep. Prog. Phys., Vol 67, pp. 1915, Apr.200
- [9] M. D. Peel, S. E. Ashbrook and P. Lightfoot, " The Polar Phase of  $\text{NaNbO}_3$ : A Combined Study by Powder Diffraction, Solid-State NMR, and First-Principles Calculations", Inorg. Chem., Vol 52, pp. 8746-8872, Jun. 2013.
- [10] D. S. Paik, S. E. Park, T. R. Shroff and W. Hackenberger, "crystallographically engineered  $\text{BaTiO}_3$  single crystals for high-performance piezoelectrics", J. Mater. Sci., Vol 34, pp.469, May.1999
- [11] H. Ghayour and M. Abdellahi, " Preparing diopside nanoparticle scaffolds via space holder method: Simulation of the compressive strength and porosity", Powder Technol., Vol 29, pp. 284, 201
- [12] H. Moradmard, S. Farjami Shayesteh, P. Tohidi, Z. Abbas and M. Khaleghi, " Structural, magnetic and dielectric properties of magnesium doped nickel ferrite nanoparticles", J. Alloys. Compd., Vol 15, pp. 30666-6, Oct.2015
- [13] E. A. Nfora Lanochee, P. A. Joy Mmu, J. N. Ghogomu and J. N. Lambi, " Structure and Magnetic Properties of Lanthanum Strontium Ferrites Nanopowders Synthesized by Thermal Decomposition of Mixed Metal Acetyl Acetonates", International Journal of Engineering Research & Technology, International Journal of Engineering Research & Technology (IJERT), Vol 4, Jul. 2015
- [14] Saeid Jabbarzare, Majid Abdellahi, Hamid Ghayour, Asiye Arpanahi and Amirshar Khandan, "A study on the synthesis and magnetic properties of the cerium ferrite ceramic", Journal of Alloys and Compounds., Vol 694, pp.800807, Oct.2017
- [15] Shivendra Kumar Jaiswal, Vijay Kumar Kashyap and Jitendra Kumar, " On the sol-gel synthesis and characterization of strontium ferrite ceramic Material", Materials Research Bulletin., Vol47, pp.692-699, Dec.2012.



10.22214/IJRASET



45.98



IMPACT FACTOR:  
7.129



IMPACT FACTOR:  
7.429



# INTERNATIONAL JOURNAL FOR RESEARCH

IN APPLIED SCIENCE & ENGINEERING TECHNOLOGY

Call : 08813907089  (24\*7 Support on Whatsapp)